Why do some post-tropical cyclones impact europe?

Article

Published Version

It is advisable to refer to the publisher's version if you intend to cite from the work. See [Guidance on citing](#).

www.reading.ac.uk/centaur

CentAUR

Central Archive at the University of Reading

Reading's research outputs online

Why Do Some Post-Tropical Cyclones Impact Europe?

ELLIOTT M. SAINSBURY,[a] REINHARD K. H. SCHIEMANN,[b] KEVIN I. HODGES,[b] ALEXANDER J. BAKER,[b]
LEN C. SHAFFREY,[b] AND KIERAN T. BHATIA[c]

[a] Department of Meteorology, University of Reading, Reading, Berkshire, United Kingdom
[b] National Centre for Atmospheric Science, University of Reading, Berkshire, United Kingdom
[c] Guy Carpenter, New York, New York

ABSTRACT: Post-tropical cyclones (PTCs) can bring high winds and extreme precipitation to Europe. Although the structure and intensity of observed Europe-impacting PTCs has been investigated in previous studies, a quantitative understanding of the factors important for PTCs to reach Europe has not been established. By tracking and identifying the full life cycle of tropical cyclones (TCs) in the ERA5 reanalysis, we investigate why some PTCs impact Europe and why others do not, using a composite analysis. We show that PTCs that impact Europe are typically ~4–6 m s^{-1} stronger at their lifetime maximum intensity and throughout the extratropical transition process. They are also twice as likely to reintensify in the midlatitudes. During ET, the Europe-impacting PTCs interact more strongly with an upstream upper-level trough in a significantly more baroclinic environment. The Europe-impacting PTCs are steered on a more poleward trajectory across a midlatitude jet streak. It is during the crossing of the jet that these cyclones often undergo their reintensification. Using contingency table analysis, TC lifetime maximum intensity, and whether post-ET reintensification occurs are shown to be significantly associated with the odds that a PTC reaches Europe. This supports our composite analysis and further indicates that TC intensity and reintensification both modulate the likelihood that a PTC will impact Europe.

SIGNIFICANCE STATEMENT: Some post-tropical cyclones (PTCs) reach Europe, often associated with extreme precipitation and high winds. It is currently unclear what factors allow this to occur. In this study, we track cyclones in two reanalyses using a feature tracking scheme and identify the PTCs by matching (in space and time) reanalysis tracks with observed tracks. Using a composite analysis, we show that 1) tropical cyclones (TCs) that are more intense, and 2) TCs that reintensify after extratropical transition, are more likely to reach Europe. TCs that reintensify interact strongly with an upper-level upstream trough and cross a midlatitude jet streak. Reintensification occurs as the cyclones cross this jet streak.

KEYWORDS: Europe; North Atlantic Ocean; Extratropical cyclones; Extratropical transition; Hurricanes/typhoons; Tropical cyclones

1. Introduction

Tropical cyclones (TCs) which enter the midlatitudes often transition from symmetric, warm-core systems into cold-core, asymmetric extratropical cyclones during a process known as extratropical transition (ET). After ET, these post-tropical cyclones (PTCs) can bring extreme wind, precipitation and waves to regions far removed from the tropics (Evans et al. 2017; Jones et al. 2003). Ex-Hurricanes Debbie (1961) (Graham and Smart 2021) and Ophelia (2017) (Stewart 2018; Rantanen et al. 2020) both set national wind speed records in Ireland. Across Scotland in 2011, ex-Hurricane Katia (Grams and Blumer 2015) was responsible for over GBP 100 million in

damages due to extreme winds, and farther east across Europe, ex-Hurricane Debby (1982) caused severe damage over northern Finland (Laurila et al. 2020). PTCs are also climatologically associated with higher intensities over Europe than midlatitude cyclones. PTCs impacting Northern Europe are typically 3.5 m s^{-1} stronger in terms of their maximum 10-m wind speed, and 10 hPa deeper, than the midlatitude cyclones that impact the region during the hurricane season (Sainsbury et al. 2020).

Climatological assessments of PTCs and their impacts over Europe have been documented in previous studies. Baker et al. (2021) show that approximately 10% of cyclones with tropical Atlantic origin impact Europe, and those retaining or redeveloping warm-core characteristics often have higher wind speeds over Europe. These cyclones often attain their lowest sea level pressure a day after impacting Europe, enhancing their destructive potential (Dekker et al. 2018). These studies improve our understanding of the characteristics and

---

impacts associated with PTCs across Europe and are a crucial addition to the ET climatologies constructed for the North Atlantic more broadly (e.g., Hart and Evans 2001; Bieli et al. 2019; Studholme et al. 2015). However, their focus is not on why, or how, these PTCs reach Europe. A quantitative understanding of the factors important for these systems to reach Europe has not been established and is addressed in this study.

Many previous studies investigate the TC–midlatitude flow interaction associated with the downstream impacts of ET, and this interaction also has implications for the transitioning cyclone itself (Jones et al. 2003; Keller et al. 2019). If the transitioning TC recurves relative to an upstream trough, the advection of anticyclonic potential vorticity by the divergent outflow of the cyclone can lead to local jet streak development, downstream ridge building, and the amplification of a downstream Rossby wave packet (Riemer et al. 2008; Riemer and Jones 2010; Archambault et al. 2013; Riboldi et al. 2019; Keller 2017). Climatologically, ET-related flow amplification is greater in the western North Pacific than in the North Atlantic (Torn and Hakim 2015; Quinting and Jones 2016); however, North Atlantic ET events have also been associated with downstream high-impact weather (Grams and Blumer 2015; Pohorsky et al. 2019), downstream flow amplification (Quinting and Jones 2016; Brannan and Chagnon 2020) and a reduction in downstream predictability (Anwender et al. 2008; Pantillon et al. 2013, 2015, 2016). Advection of midlatitude potential vorticity by the outflow anticyclone associated with a transitioning TC can lead to a local deceleration of the upstream trough (Agusti-Panareda et al. 2004; Archambault et al. 2015; Keller et al. 2019), leading to a prolonged period of favorable phasing (phase-locking) between the transitioning TC and the midlatitude waveguide and additional downstream flow amplification.

The TC–trough interaction conducive for downstream amplification also favors reintensification of the transitioning TC (Klein et al. 2000; Keller et al. 2019; Grams et al. 2013a,b). TCs which recurve relative to an upstream trough (the northwest pattern, Harr et al. 2000) are typically steered on a more poleward trajectory and are much more likely to undergo reintensification in the midlatitudes, with reintensification enhanced by increases in eddy heat flux (Harr et al. 2000). In the North Atlantic, an association has previously been found between reintensification post-ET and interaction with a negatively tilted (northwest to southeast) trough. The negative tilt permits the cyclone a closer approach to the trough and is associated with a contraction and increase in eddy potential vorticity toward the center of the transitioning TC (Hart et al. 2006), although more recent work suggests that the negative tilt may be a consequence of strong TC–trough interaction, rather than a predictor for future PTC outcomes (Sarro and Evans 2022). Many climatological studies of PTC evolution are focused around TCs in the western North Pacific (e.g., Harr et al. 2000; Klein et al. 2000, 2002), with much focus on case studies in the North Atlantic (e.g., McTaggart-Cowan et al. 2001, 2003, 2004; Agusti-Panareda et al. 2004). As far as the authors are aware, Hart et al. (2006) is the only published study on the climatological factors determining post-ET

evolution of PTCs. However, it uses a very small sample size, with 6 reintensifying cyclones and 11 weakening cyclones. To generalize the results from case studies, an updated climatology for the North Atlantic basin is necessary.

Not only are PTCs disproportionately responsible for high-impact windstorm risk in the current climate (Sainsbury et al. 2020), their frequency and intensity across Europe may also increase in the future due to climate change (Haarsma et al. 2013; Baatsen et al. 2015). However, accurately simulating PTCs can be challenging for CMIP-class climate models due to their coarse resolution (Davis 2018). Many climate models are unable to accurately simulate TC genesis and intensity, which are likely to be important for simulating PTC statistics. Even high-resolution climate models, such as used in Haarsma et al. (2013) are not sufficient to simulate the strongest TCs (Vidale et al. 2021). If a good physical understanding can be established surrounding the factors which are important for PTCs to reach Europe, and how these factors will change because of climate change, then this information can be used to inform future modeling studies on projected changes of European-impacting PTCs.

European-impacting PTCs generally recurve near the U.S. East Coast (i.e., Fig. 1b in Baker et al. 2021) and often travel across the entire North Atlantic before they reach Europe. Longevity is therefore key to their ability to reach Europe. We hypothesize two influences for PTC longevity, related to 1) the tropical environment in which the storm originates and resides as a TC, and 2) the midlatitude environment that the TC transitions into. On point 1), a very strong TC which recurves into the midlatitudes will have a stronger warm-core structure, which may be consistent with increased resilience to hostile midlatitude conditions. This could potentially allow the TC to survive longer and reach Europe. Previous studies have highlighted that stronger North Atlantic TCs are able to endure hostile conditions for longer. Hart and Evans (2001) show that weak TCs only tend to reintensify post-ET if they have a transit time of less than 20 h between a region favorable for tropical cyclogenesis (potential intensity < 960 hPa) and a region favorable for extratropical cyclogenesis (Eady growth rate > 0.25 day^{-1}). However, two-thirds of strong TCs (minimum sea level pressure < 970 hPa) that reintensify endured more than 20 h of transit time. On point 2), if the midlatitude environment into which the TC recurves and transitions is favorable for reintensification, then the PTC will likely reintensify, extending the length of the PTC's life. We therefore hypothesize that PTCs which interact strongly with an upstream trough in a baroclinic environment will be more likely to reach Europe, as this interaction of favorable for reintensification (e.g., Klein et al. 2000; Harr et al. 2000; Riboldi et al. 2019).

In this paper, we investigate whether there are differences in cyclone and environmental characteristics between PTCs which do, and do not, reach Europe. This is achieved by creating an updated climatology of PTCs. By separating PTCs based on whether they impact Europe, we can use a composite analysis to investigate whether Europe-impacting PTCs are more intense in the tropical phase of their life cycle, or

reintensify more post-ET, than PTCs which do not reach Europe.

The paper continues in section 2 with a description of the data and methodology. Section 3 contains a composite analysis of PTCs that do and do not impact Europe, along with an evaluation of which factors may be important for a PTC to impact Europe. The paper concludes with a discussion in section 4.

2. Data and methods

The TC tracks in the Hurricane Database version 2 (HURDAT2; Landsea and Franklin 2013) often only contain position and intensity information for storms during the time period for which they were operationally designated as TCs (Hagen et al. 2012; Delgado et al. 2018), with post-ET information sparse and incomplete. This makes it impossible to analyze the trajectories of PTCs in the midlatitudes without considering other datasets and methodologies. In this study, we track all cyclones in the European Centre for Medium-Range Weather Forecasts Reanalysis version 5 (ERA5) using a feature tracking scheme and identify the observed TCs by performing a spatiotemporal track matching to HURDAT2. Both steps are described in more detail in sections 2b and 2c. This methodology gives us the full life cycle, including the cyclones post-tropical evolution and trajectory through the midlatitudes.

a. Data

The ERA5 (Hersbach et al. 2020) reanalysis provides the environmental fields for analysis and the geopotential height fields used for cyclone phase space (CPS; Hart 2003) parameter calculation (300, 600, 900 hPa). Relative vorticity fields from 600 to 850 hPa are also used for cyclone tracking. All data used are 6-hourly. ERA5 has a horizontal resolution of T639 (~30 km in the midlatitudes) and uses 4D-Var data assimilation provided by cycle 41R2 of the ECMWF Integrated Forecasting System, which was operational in 2016. ERA5 data from 1979 to 2018 are used.

Observational best track TC data from HURDAT2 are used for objective track matching and to provide realistic wind and pressure data for the tropical phase of the cyclones, as reanalyses underestimate the intensity of TCs due to their insufficient horizontal resolution (Hodges et al. 2017).

b. Cyclone detection and tracking

We use TRACK (Hodges et al. 2017) to track the cyclones through the ERA5 reanalysis. This is achieved by first vertically averaging the 600–850-hPa relative vorticity and spectrally filtering to a T63 (~180 km) resolution. The planetary scales are also removed (waves with wavenumbers < 6). Features with a vorticity anomaly exceeding 0.5×10^{-5} s^{-1} are then initialized into tracks using a nearest neighbor method. These tracks are refined by minimizing a cost function for track smoothness, forwards and backward in time, subject to adaptive constraints for track smoothness and displacement distance in a time step. Cyclones lasting for longer than 2 days are retained for further analysis. This method allows us to obtain the full life cycles of all cyclones (tropical and extratropical) in the ERA5 reanalysis. The cyclones forming in the North Atlantic basin are then selected.

Mean sea level pressure (MSLP) minima are attached to each track for each 6-hourly time step by sampling the full resolution MSLP reanalysis data along the cyclone tracks. The nearest pressure minima within a 5° radius (geodesic) spherical cap of the vorticity center is used, which is determined using B-spline interpolation and steepest descent minimization. The maximum 10-m winds in a 6° cap of the vorticity center are identified using a direct grid point search and are also added to the tracks.

c. Objective track matching

To identify which of the tracked cyclones correspond to the observed TCs, we employ objective track matching. The methodology is the same as described in Sainsbury et al. (2020), Sainsbury et al. (2022) and Hodges et al. (2017). A reanalysis cyclone track matches a track in HURDAT2 (and thus is designated as a TC) if the mean separation distance between the tracks is less than 4° (geodesic) over the time period for which the cyclones overlap. If there is more than 1 cyclone track in the reanalysis meeting this criterion, then the track with the smallest mean separation distance to the HURDAT2 track is designated as a TC. This method to identify TCs in reanalyses gives us information on the position and intensity of the TCs from the time at which the vorticity anomaly first forms until it has completely decayed. Unlike the TC tracks in HURDAT2, this therefore gives us detailed information on the precursor and post-tropical stages of the TC life cycle.

TCs tracked through ERA5 are identified as PTCs if they enter a region in the North Atlantic midlatitudes over 36°–70°N and 70°W–30°E and complete ET (section 2d). PTCs are further designated as "Europe PTCs" if they enter the domain 36°–70°N, 10°W–30°E, or "NoEurope PTCs" if they enter the PTC domain and complete ET, but do not impact the "Europe" region. These regions are constructed such that all European impacting PTCs are defined as PTCs, as the European domain is wholly contained within the PTC domain. These domains have been overlaid on Fig. 1 (black box for the PTC domain, red box for the Europe domain). During our analysis period (1979–2018), there are 60 PTCs which reach Europe, and 120 PTCs which do not. To ensure the results are robust to this difference in sample sizes, bootstrap resampling was used to generate samples of size 60 for the PTCs which do not reach Europe. This process was iterated 1000 times, and the composites reproduced for the resampled mean. The results were not sensitive to the difference in sample size (not shown).

d. Extratropical transition

TCs entering the midlatitudes often undergo extratropical transition, a process whereby the vertically stacked, symmetric cyclone loses its deep warm core and becomes asymmetric as it develops frontal features. This process can be captured objectively using the cyclone phase space (CPS) parameters described in Hart (2003). The thermal asymmetry B is calculated as

$$B = h(\overline{Z_{600} - Z_{900}}|_R - \overline{Z_{600} - Z_{900}}|_L). \tag{1}$$
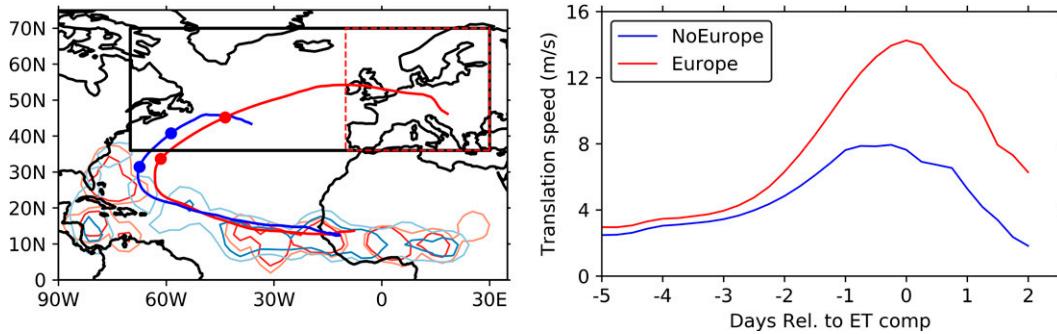
FIG. 1. (a) Composite trajectory of the Europe PTCs (red) and the NoEurope PTCs (blue), centered on ET comple-
tion. Dots represent the composite mean location of ET onset (dots outside the PTC domain) and completion (dots inside
the PTC domain). Open contours represent the genesis density (contours shown for 1 and 2 TCs per unit area per year,
where the unit area is equal to a 5° radius cap). The black box shows the PTC domain, and the red dashed box shows the
European domain. (b) The composite mean translation speed for the two composites centered on ET completion.

In Eq. (1), Z represents the geopotential height on the pres-
sure surface given by the subscript, and overbar denotes the
area mean over a semicircle relative to the cyclone's direction
of travel (R = to the right, L = to the left), within a cap with
radius of 5° (geodesic), $h = 1$ in the Northern Hemisphere, -1
for the Southern Hemisphere.

The lower ($-|V_T^L|$) and upper ($-|V_T^U|$) tropospheric thermal
wind around the cyclone are calculated as follows:

$$-|V_T^L| = \frac{\partial(\Delta Z)}{\partial \ln p}\Big|_{600\text{hPa}}^{900\text{hPa}}, \tag{2}$$

$$-|V_T^U| = \frac{\partial(\Delta Z)}{\partial \ln p}\Big|_{300\text{hPa}}^{600\text{hPa}}, \tag{3}$$

where $\Delta Z = Z_{\max} - Z_{\min}$ and $Z_{\max}$, $Z_{\min}$ are the maximum
and minimum geopotential heights, respectively, at a given
pressure level within a 5° (geodesic) cap about the cyclone
center. Positive values of $-|V_T|$ indicate a warm core in the
tropospheric region of the cyclone, and negative values indi-
cate a cold core.

Positive values for lower and upper-level thermal wind in
conjunction with a B value of <10 m indicate systems are
non-frontal and have a deep warm core. The beginning of
transition, ET onset, is defined as the time at which the cy-
clone loses its lower-level warm core or becomes thermally
asymmetric ($B > 10$ m or $-|V_T^L| < 0$). ET completion is then
defined when both criteria are met, i.e., the low-level thermal
wind becomes negative, and B exceeds 10 m.

Note that some TCs, particularly very weak ones, never at-
tain a symmetric, deep warm-core structure in the reanalyses
($-|V_T^L|$ and $-|V_T^U|$ never both > 0, B never < 10). As these
TCs never meet the CPS criteria for a TC to begin with, they
cannot start, or complete ET. Therefore, these cyclones are
excluded from the analysis. While tropical depressions and
subtropical cyclones are not strictly excluded from our analy-
sis, they rarely meet the CPS criteria, and therefore cannot
complete ET and are also excluded. Table 1 documents the
sample size for PTCs (TCs which both enter the PTC domain
and complete ET in ERA5). Data from the third column are

used for the intensity analysis of section 3b (and in Fig. 10b),
and data from the second column are used for all other analy-
sis presented.

e. Storm-centered composite methodology

To investigate the midlatitude environment around PTCs
which do and do not impact Europe, a storm-centered com-
posite methodology is used. This is the same method as used
in Bengtsson et al. (2007), Catto et al. (2010) and Dacre et al.
(2012). Data in a cap of pre-specified radius around the cy-
clone are extracted from the full field onto a radial coordinate
system that is centered on the cyclone (initially centered on
the pole and then rotated to the storm center). This is done to
avoid problems associated with changes in grid spacing across
the sphere. In section 3c(1), storms are oriented based on
their propagation direction, however in sections 3c(2) and 3d,
they are not. This is because in section 3c(1) we focus our
analysis on the cyclone structure, whereas in sections 3c(2)
and 3d we are interested in the environment surrounding the
cyclones. For more information on this storm-centered com-
posite method, see the appendix of Bengtsson et al. (2007).

f. Statistical significance

Significance of results is calculated using a two-sample
Kolmogorov–Smirnov test to compare the distributions of
the Europe and NoEurope PTCs. [To account for spatial

TABLE 1. Sample sizes for the Europe, NoEurope, and total
(Europe + NoEurope) PTCs considering: all storms tracked in
the ERA5 reanalysis with a matching TC in HURDAT2 that
complete ET in ERA5 and enter the PTC domain (black box in
Fig. 1) (second column), and those that at the time step of ET
completion in the reanalysis still have observational data available
in HURDAT2 (third column, which is the basis for Fig. 2).

	PTCs	HURDAT2 obs available at designated ET completion time
Europe	60	47
NoEurope	120	87
Total	180	134

correlations in Figs. 3, 4, and 7, the methodology of Wilks (2016) is also employed to account for the false discovery rate, using $\alpha_{FDR} = 0.05$.] This leads to the null hypothesis (no difference between Europe and NoEurope PTCs) being rejected less frequently than when simply assuming significance if the p value for the null hypothesis is less than 0.05.

g. Eady growth rate and potential vorticity diagnostics

To investigate whether there are differences in the baroclinicity surrounding the two PTC composites, the Eady growth rate σ (Hoskins and Valdes 1990) is calculated as in previous studies (Liu et al. 2017; Baker et al. 2022). The Eady growth rate is defined as

$$\sigma = 0.31 \frac{f}{N} \frac{\partial U}{\partial z}, \qquad (4)$$

where f is the Coriolis parameter, N is the Brunt–Väisälä frequency, $U = U(u, v)$ is the zonal and meridional components of the horizontal wind, and z is the isobaric height. Vertical derivatives for z and the horizontal wind are calculated between the 250- and 850-hPa isobaric height surfaces using 6-hourly ERA5 data.

The interaction between a transitioning TC and an upper-level trough is associated with downstream ridge building and jet streak amplification (e.g., Keller et al. 2019), which is largely the result of negative PV advection associated with the TC's divergent outflow (Riemer et al. 2008; Grams et al. 2013a; Pantillon et al. 2013). TC–trough interaction also plays a crucial role in whether the transitioning TC subsequently reintensifies after ET (Hart et al. 2006; Riboldi et al. 2019). To quantify the interaction between transitioning TCs and upstream troughs, the negative potential vorticity advection by the irrotational wind (Archambault et al. 2013):

$$PV_{irrot} = -\mathbf{V}_\chi \cdot \nabla_P PV, \qquad (5)$$

is calculated using 6-hourly ERA5 data. Potential vorticity and horizontal winds are averaged between 250 and 350 hPa. The wind is decomposed into irrotational and rotational components using a Helmholtz partition as in previous studies (Quinting and Jones 2016; Riemer et al. 2008). Both σ and PV_{irrot} are averaged in a 15° cap centered on the cyclone during ET for comparison between the composites.

3. Results

Here we present a composite analysis of the Europe-impacting PTCs (hereafter referred to as "Europe PTCs"), and the PTCs which do not impact Europe (hereafter called "NoEurope PTCs"). We first investigate differences in the composite mean TC trajectories and the role of TC intensity, followed by differences in the cyclones and environment about the point of extratropical transition (ET). Analysis centered about the point of extratropical reintensification post-ET is then presented, followed by analysis of the relative importance of the differences between the composites.

a. Cyclone trajectory

The composite trajectories for the Europe and NoEurope PTCs are first plotted to investigate whether there are differences in the location of recurvature, and to understand how the trajectories differ in the midlatitudes. The composite trajectories are constructed using the average location of all Europe and NoEurope PTCs at each time step, centered about the point of ET completion. This is presented in Fig. 1a. A 1-day running mean is used to smooth the cyclone tracks before compositing, and the composite trajectory is only shown for the time steps for which there are at least 10 TCs still present.

Both the Europe and NoEurope PTCs tend to start in similar locations over West Africa, where the seeds for many strong TCs exist as African easterly waves (Landsea 1993; Russell et al. 2017; Thorncroft and Hodges 2001). The Europe PTCs recurve and enter the PTC domain approximately 5° farther east in the basin. The largest differences between the composites are the position of ET completion, and the post-ET trajectory of the composites. The NoEurope PTCs travel northeastward in the midlatitudes after entering the PTC domain, attaining an average maximum latitude of approximately 45°N. The Europe PTCs continue to gain latitude as they cross the Atlantic, reaching ~55°N while over Europe. This may allow the Europe PTCs to enter a more baroclinic environment, aiding extratropical reintensification as the cyclones recurve and travel toward Europe. Genesis densities show no difference in the genesis location of the PTCs which do, and do not impact Europe.

The Europe PTCs complete ET significantly (95%, Kolmogorov–Smirnov test) farther poleward and significantly farther eastward (15° farther east and 4.4° farther poleward) than the NoEurope PTCs. However, the difference between composite locations of ET onset is much smaller, indicating that the Europe PTCs travel a greater distance during ET, possibly indicating that the westerlies in the vicinity of the Europe PTCs are stronger than for NoEurope PTCs. The Europe PTCs undergo greater acceleration during ET than NoEurope PTCs (Fig. 1b), consistent with the stronger temperature gradients (shown in Fig. 3). There is also a distinct difference in seasonality of the Europe and NoEurope composites. Only 15% of PTCs which complete ET in June reach Europe; however, 50% of PTCs completing ET in November reach Europe (Fig. S1 in the online supplemental material). There is no significant difference in the length of ET between the composites (2.1 and 2.0 days for Europe, NoEurope PTCs, respectively).

The NoEurope PTCs have a shorter lifespan in the midlatitudes, and as a result, do not make it as far east as the Europe PTCs. This confirms that longevity is crucial in determining whether a PTC will impact Europe, as the NoEurope PTCs dissipate on approach. The mean midlatitude translation speed, averaged over the cyclone's whole life cycle post-ET, is similar and differences are nonsignificant between both composites (12.5 and 11.7 m s^{-1} for Europe and NoEurope PTCs, respectively). However, the maximum midlatitude translation speeds differ significantly at the 95% level (23.2 and 19.5 m s^{-1} for Europe and NoEurope PTCs, respectively). This may

indicate that Europe PTCs are more likely to rapidly propagate eastward in the presence of a jet streak (and is consistent with Fig. 6).

b. The association between TC intensity and Europe-impact likelihood

To investigate which factors may influence the likelihood that a PTC will impact Europe, we first analyze the tropical phase of the cyclones. In this section, we compare the intensity of the Europe and NoEurope PTCs. Figure 2 shows the composite intensity as a function of time for the Europe (red) and NoEurope (blue) PTCs, centered about ET completion. The bottom panel shows the number of cyclones (Europe and NoEurope) which go into the composites at each time step. We use intensity data (MSLP and 10-m wind) from HURDAT2 and ERA5.

The Europe PTCs are significantly more intense (10-m wind and sea level pressure) than the NoEurope PTCs. This may be consistent with the Europe PTCs having a more resilient structure, capable of withstanding the structural changes through ET for longer as baroclinicity and shear increase, and SSTs decrease. This significant difference persists from before the time of composite mean maximum intensity until several days after ET has completed; however, the sample size decreases rapidly from the time step of ET completion onward (Fig. 2c). Overall, the significant difference persists for greater than 7 days. At the composite mean maximum intensity (Fig. 2a) and actual TC lifetime maximum intensity, the Europe PTCs are more than 5 m s^{-1} stronger than the NoEurope PTCs, and this difference increases to almost 10 m s^{-1} by 2-day post-ET completion. Figure 2 also shows a secondary peak in intensity after ET completion for the Europe PTCs, in agreement with Baker et al. (2021) (Fig. 8 therein), indicating that this post-ET intensity increase is seen across reanalyses. Furthermore, this suggests that there may be greater reintensification associated with the Europe PTCs than is associated with the NoEurope PTCs. Europe PTCs appear to reintensify more when considering the SLP (Fig. 2b) than when considering wind (Fig. 2a). This may be the result of the Europe PTCs gaining more latitude than the NoEurope PTCs, entering a region of lower climatological background pressure. However, as there are indications of reintensification in the wind data (Fig. 2a), it is likely that the Europe PTCs are undergoing some reintensification, which is confirmed in sections 3d and 3e. Intensity estimates from ERA5 (dashed lines, Figs. 2a and 2b) before ET completion should be treated with caution, as reanalyses do not have sufficient resolution to capture the structure and intensity of TCs (Hodges et al. 2017). ERA5 is included to check whether there is agreement with observational HURDAT2 data post-ET completion, which is necessary if we wish to rely on ERA5 for cyclone analysis in section 3c onward. We see qualitative agreement with HURDAT2, with ERA5 data indicating that Europe PTCs are significantly more intense than the NoEurope PTCs throughout their life cycle, with further signs of possible reintensification of Europe PTCs in Fig. 2b.
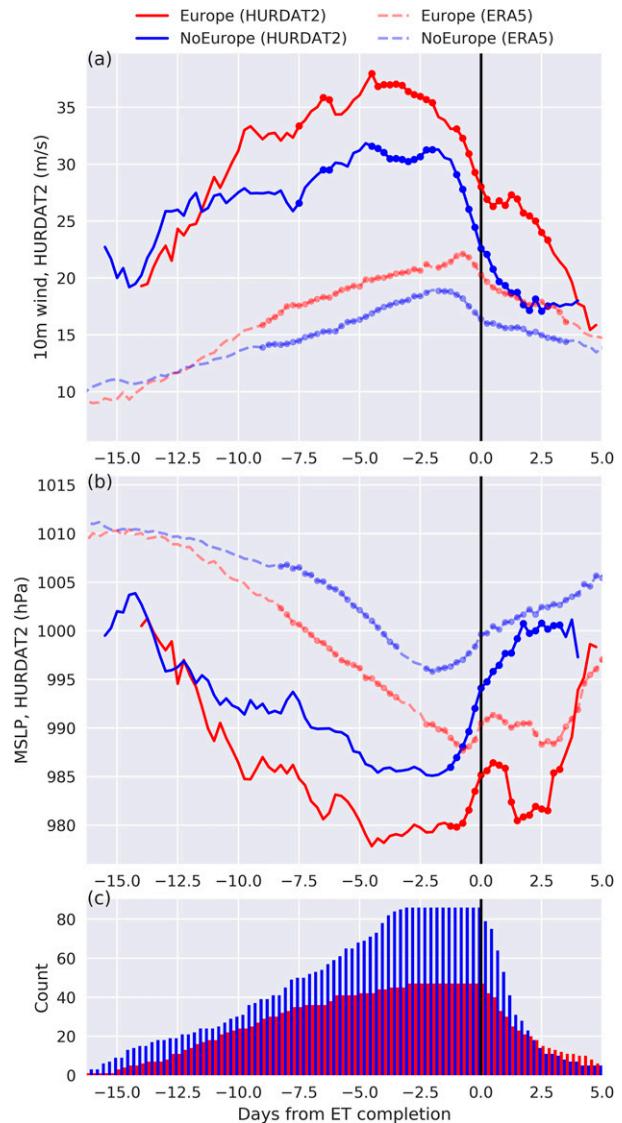

FIG. 2. Composite life cycle of the intensity of the Europe (red) and NoEurope PTCs (blue): (a) for 10-m wind and (b) for MSLP for HURDAT2 (solid lines) and ERA5 (dashed lines). (c) The sample sizes for the HURDAT2 data. Dots overlaid represent the time steps at which the difference in the intensities is significant to 95%.

c. Composite evolution of storm structure and surrounding environment

1) EVOLUTION OF STORM STRUCTURE

In this section we investigate the structure of the cyclone-centered composites of the Europe and NoEurope PTCs. This analysis aims to assess whether differences in cyclone characteristics exist, and if they do exist, whether they are consistent with our hypothesis that PTCs which reintensify are more likely to reach Europe. Figure 3 shows a 48-h evolution of the 850-hPa temperature in a 20° cap around the cyclones, centered on the completion of ET. For each cyclone, the anomaly is calculated by subtracting the mean 850-hPa
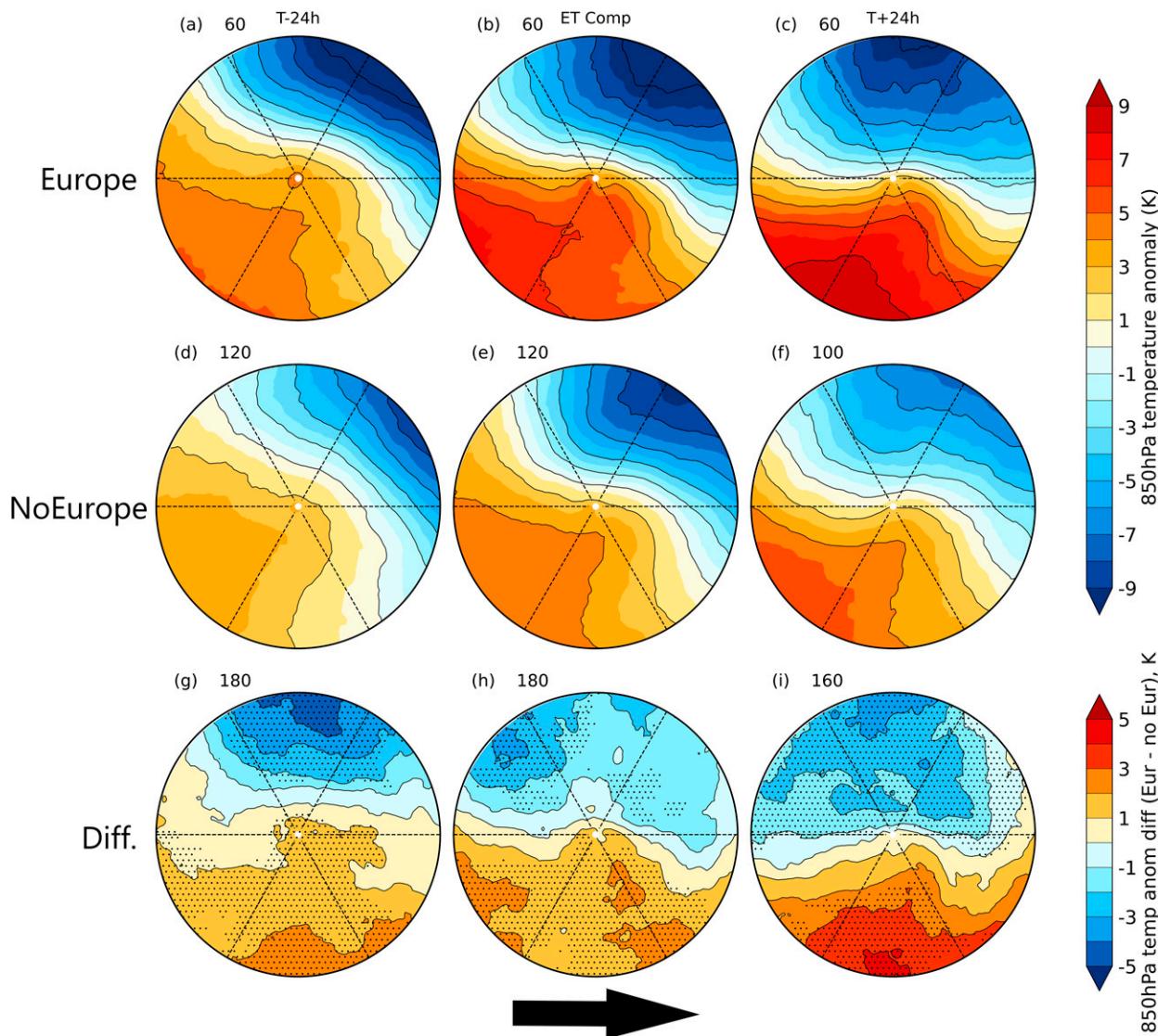
FIG. 3. Storm-centered composite (20° cap) of the 850-hPa temperature anomaly (850-hPa temperature minus the 20° cap radial mean 850-hPa temperature) for (a)–(c) the Europe PTCs and (d)–(f) the NoEurope PTCs, and (g)–(i) the difference (Europe minus NoEurope). Plots show a 48-h evolution, centered about the point of ET completion. Cyclones are aligned according to their direction of travel before compositing, so that they move from west to east in the composite. In (g)–(i), stippling denotes the regions in which the differences are significant to 95%. The large arrow shows the direction of storm propagation. Sample size shown in the upper left of each panel.

temperature over the 20° cap before the compositing is applied. The cyclones are oriented based on their propagation direction, such that the cyclones are moving west to east in the composite.

During the 48-h period centered on ET completion, the composite mean temperature gradient is much larger for the Europe PTCs than the NoEurope PTCs. The 850-hPa temperature range in a 10° cap about the cyclone center is 74%, 27%, and 54% greater for the Europe PTCs than the NoEurope PTCs at 24 h prior to ET completion, at ET completion, and 24 h after ET completion, respectively. This may be associated with the difference in location of the Europe and NoEurope

PTCs throughout this stage in the cyclone's life cycle shown in Fig. 1.

Differencing (Europe minus NoEurope) the cyclone composites highlights significant differences (Figs. 3g–i). The Europe PTCs are associated with statistically significantly cooler 850-hPa temperatures to the left of the cyclone's propagation direction than the NoEurope PTCs. These cyclones mainly travel from west to east (or from southwest to northeast), and so the area above of the cyclone center in Fig. 3 is likely to represent the region poleward of the cyclones. Considering the absolute 850-hPa temperatures, the Europe PTCs have significantly colder temperatures to the left of their propagation
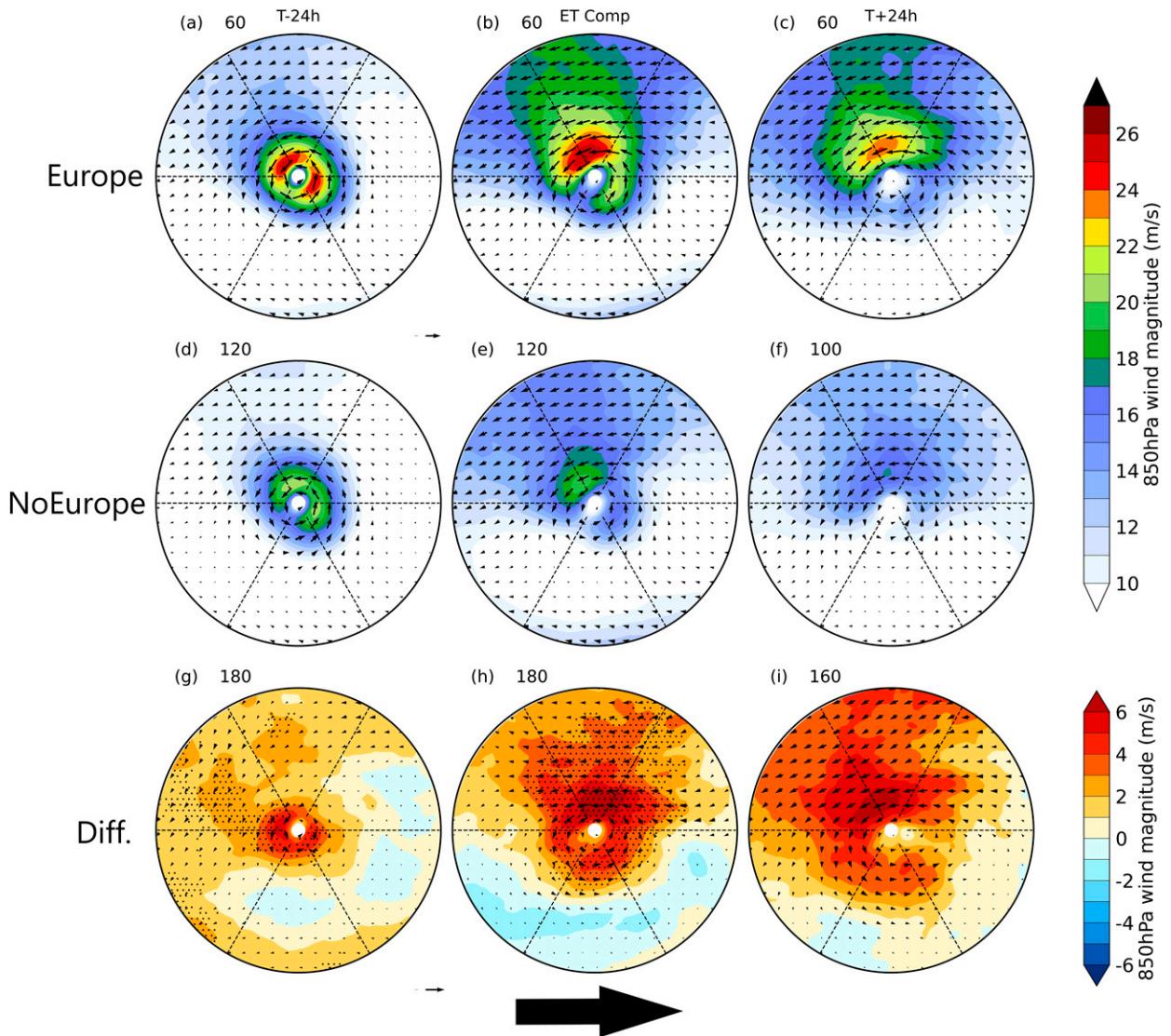
FIG. 4. As in Fig. 3, but for the storm-relative 850-hPa wind magnitude (and direction). A 10° cap is used. Storm-relative winds are calculated by subtracting the translation velocity from Earth-relative winds. Key length is equal to 20 m s^{-1} for (a)–(f) and 10 m s^{-1} for (g)–(i). In (g)–(i), stippling indicates the region in which the difference in the composite means is significant to 95%. Cyclones are aligned according to their direction of travel before compositing, so that they move from west to east in the composite. The large arrow shows the direction of storm propagation. Sample size is shown in the upper left of each panel.

direction, but similar temperatures in the warm sector, despite the Europe PTCs being ∼5° farther poleward (not shown). This suggests that Europe PTCs are associated with considerably stronger warm air advection, and highlights that the enhanced temperature gradient accompanying the Europe PTCs is likely associated with the differences in position (Fig. 1a) and seasonality (Fig. S1) between the composites.

Figure 4 is equivalent to Fig. 3 but instead shows the 850-hPa cyclone-relative wind magnitude and direction. As with Fig. 3, cyclones are oriented based on their propagation direction before compositing. Cyclone relative wind magnitude and direction are calculated by subtracting the translation velocity from Earth-relative winds.

The features of ET established in recent studies (e.g., Evans et al. 2017) can be seen. Over the 48-h period centered on ET completion, the wind field expands considerably, and asymmetry in the wind field grows as the cyclones in the composites lose their warm core and begin to develop frontal features in the presence of increasing shear and decreasing SSTs. The strongest winds are to the left of the cyclones (relative to propagation direction) from ET completion onward, indicative of the cold conveyor belt of extratropical cyclones (Catto et al. 2010).

During ET, the Europe PTCs are associated with significantly higher 850-hPa wind speeds than the NoEurope PTCs. This difference is significant, at 95% (indicated by the stippling),

TABLE 2. A summary of the composite mean maximum intensity, gale-force wind area (>17 m s^{-1}, Beaufort scale 8), and strong gale area (>21 m s^{-1}, Beaufort scale 9) for the Europe PTCs, NoEurope PTCs, and the percentage differences. Areas are expressed as $\times 10^3$ km^2. Values within a 10° cap of the cyclone center are considered. Percentage differences in area of strong winds are only calculated where there is sufficient area in both composites to produce a reliable percentage difference.

	Max wind magnitude			Area > 17 m s^{-1}			Area > 21 m s^{-1}		
	$T - 24$	ET	$T + 24$	$T - 24$	ET	$T + 24$	$T - 24$	ET	$T + 24$
Europe	25.2	26.1	24.2	296	1089	896	130	186	126
NoEurope	20.8	19.8	17.1	166	139	4	0	0	0
Difference	21%	32%	42%	78%	683%	—	—	—	—

close to the cyclone center, extending further from the center in the upper-left section of the composite cyclone (Figs. 4g,h), where the strongest winds exist. In Figs. 4i and 4p values are less than 0.05 around and above the cyclone, but these values are nonsignificant when accounting for spatial correlations between grid points using the false discovery rate. The Europe PTCs have maximum 850-hPa winds 21%, 32%, and 42% higher than the NoEurope PTCs 24 h prior to ET completion, at ET completion, and 24 h after ET completion, respectively. This indicates that the Europe composite contains stronger cyclones than the NoEurope composite. The area covered by with gale-force (Beaufort scale 8, >17 m s^{-1}) winds is considerably larger for the Europe PTCs than the NoEurope PTCs, and the percentage difference increases from 24 h prior to ET completion to 24-h post-ET completion. Table 2 contains a summary of the maximum wind magnitude, gale-force wind area, and strong gale-force wind area (along with differences) for the composites.

The evolution of the thermal structure of the two composites is investigated by analyzing the trajectory through the CPS. This is shown in Fig. 5. The composite trajectories through the phase space are created by centering the cyclones about the point of ET completion and applying a 2-day running mean to smooth the trajectory. This is longer than the running mean used in Fig. 1 but is necessary because the data comprising Fig. 5 are noisier than the position information used in Fig. 1.

A large difference between the composites is found in the B parameter. The Europe PTCs (red line) have a maximum thermal asymmetry (B) value which is ~70% larger than for the NoEurope PTCs (Fig. 5a). The difference in B at ET completion is statistically significant to 95%. This suggests that the Europe PTCs develop stronger frontal features than the NoEurope PTCs. The significantly larger B parameter associated with Europe PTCs could also indicate that the Europe PTCs are embedded in a region of higher baroclinicity than the NoEurope PTCs, highlighting the importance of the composite mean differences in cyclone location (Fig. 1a) and seasonality (Fig. S1). The Europe PTCs attain higher values for
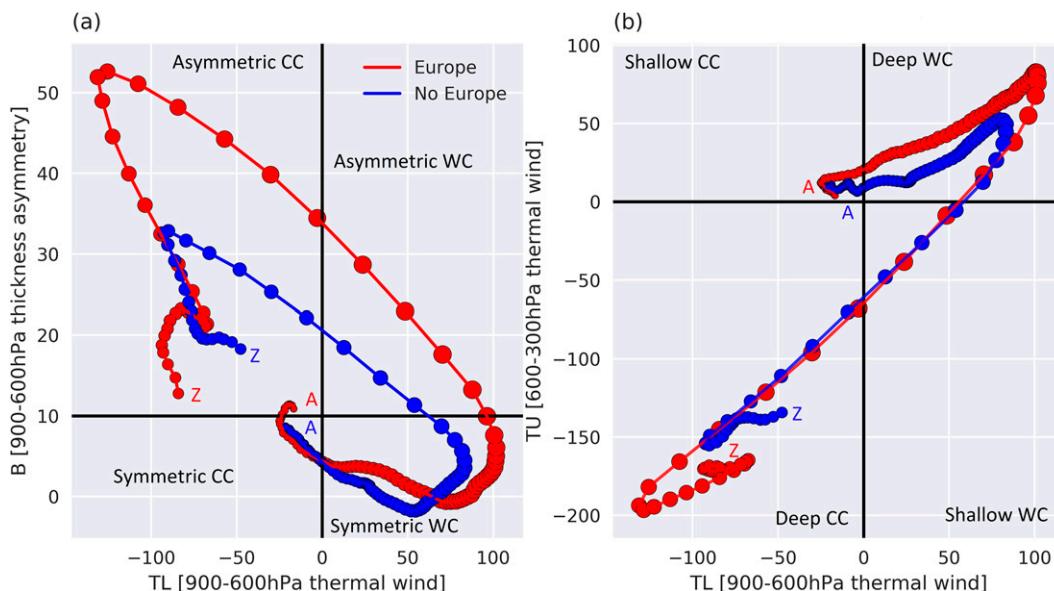

FIG. 5. Composite life cycle through the cyclone phase space planes for the Europe (red) and NoEurope (blue) PTCs. Composites are centered about the point of ET completion. The letters A and Z represent the phase space location of the composites at the beginning and end of their life cycle, respectively. Composite mean 10-m wind speed at each time step from ERA5 is illustrated using the size of the markers.
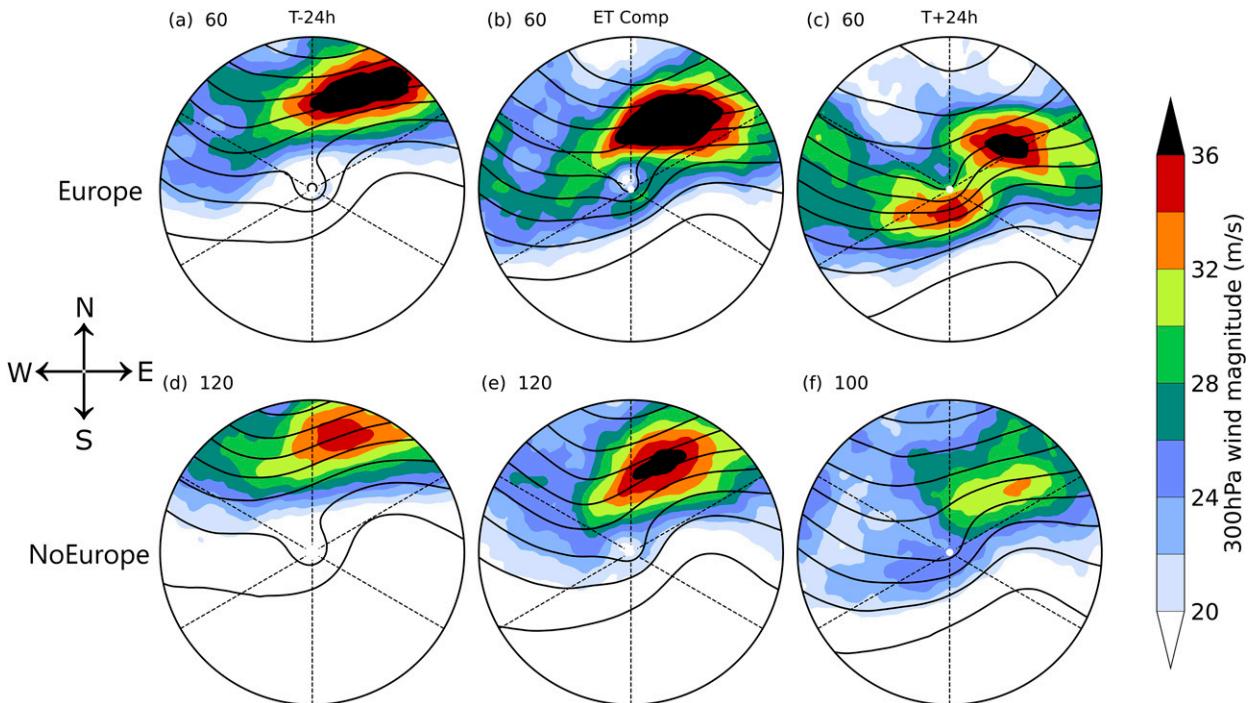
FIG. 6. Storm-centered composites (20° cap) of the 300-hPa wind magnitude (filled contours) and 500-hPa geopotential height (black open contours) for (a)–(c) the Europe and (d)–(f) NoEurope PTCs. The 48-h evolution centered about the point of ET completion. Cyclones are not aligned based on their direction of travel. Sample size is shown in the upper left of each panel.

the lower and upper-level thermal wind at their maximum intensity, though the difference is not statistically significant (Fig. 5b). Larger upper and lower-level thermal wind values suggests a stronger deep warm core, indicating a stronger TC. Consistent with Fig. 4, which shows that the Europe TCs have stronger winds after ET, the CPS trajectories indicate that the Europe TCs undergo more extratropical reintensification in the mid latitudes. This extratropical reintensification may be the cause of the longer post-ET life cycle of Europe TCs (6.25 and 3.75 days for Europe and NoEurope PTCs, respectively), potentially allowing the cyclones to reach Europe.

2) EVOLUTION OF LOCAL ENVIRONMENT

The analysis of section 3c(1) suggests that Europe PTCs are more intense than NoEurope PTCs, and reintensify more than NoEurope PTCs post-ET. In this section, we investigate the environment surrounding the Europe and NoEurope PTCs to understand why these differences in reintensification exist. As we are looking at the environment around the cyclones, we do not align cyclones along their propagation directions in the construction of the composites in this section.

Figure 6 shows the storm-centered composite of the 300-hPa Earth-relative wind magnitude (the approximate level of the jet) and 500-hPa geopotential height in a 20° cap around the cyclone center over a 48-h period centered on ET completion. At 24 h prior to ET completion, the Europe PTCs are situated closer to an upstream trough than the NoEurope PTCs. At this time, negative PV advection by the irrotational wind (Archambault et al.

2013, 2015) is significantly higher for the Europe PTCs than the NoEurope PTCs, indicating a stronger interaction between the Europe composite and the upstream trough (Table 3). Negative PV advection by the irrotational wind is also associated with downstream Rossby wave amplification (Archambault et al. 2013; Grams and Blumer 2015). This is not visible in Fig. 6, and a follow up composite study centered on the time of maximum TC–trough interaction would be necessary to understand whether Europe PTCs are more likely to trigger downstream ridge building, jet streak amplification and downstream high-impact weather (e.g., Keller et al. 2019).

TABLE 3. Eady growth rate σ (day^{-1}) and negative PV advection by the irrotational wind, PV$_{irrot}$ (PVU day^{-1}; 1 PVU = 10^6 K kg^{-1} m^2 s^{-1}) averaged in a 15° cap around the center of each cyclone at 24 h prior to ET completion, ET completion, and 24-h post-ET completion for Europe PTCs and NoEurope PTCs. Differences (Europe minus NoEurope) are shown in the last column, and bold values are significant at the 95% level using a Kolmogorov–Smirnov test.

	Europe	NoEurope	Difference
$\sigma(T - 24\text{h})$	0.41	0.36	**0.05**
$\sigma(\text{ET Comp})$	0.53	0.45	**0.08**
$\sigma(T + 24\text{ h})$	0.58	0.49	**0.09**
PV$_{irrot}(T - 24\text{ h})$	0.85	0.76	**0.09**
PV$_{irrot}(\text{ET Comp})$	1.20	1.03	0.17
PV$_{irrot}(T + 24\text{ h})$	0.99	0.94	0.05

The Europe PTCs are also situated in a region of uniformly greater geopotential height gradients than the NoEurope PTCs, signaling stronger baroclinicity in the region of the Europe PTCs related to differences in the location and seasonality of the composites. This is also confirmed by Table 3, which shows that the Europe PTCs are in a region of significantly higher (95% level) Eady growth rate throughout ET completion than NoEurope PTCs. The closer approach to (and greater interaction with) the trough may steer the cyclone on a more poleward trajectory, with the cyclones recurving relative to the trough. The poleward steering of the cyclones enables the Europe PTCs to directly interact with the midlatitude jet streak on the eastward flank of the trough. This is consistent with previous studies which highlight the importance of the TC–trough interaction for post-ET reintensification and downstream impacts (Hart et al. 2006; Keller et al. 2019). It is also very similar to the northwest pattern (Harr et al. 2000; Klein et al. 2000), in which transitioning cyclones in the presence of an amplified upstream trough gain latitude as they undergo rapid extratropical reintensification. The tip of the upstream trough acts as a bifurcation point (Grams et al. 2013b; Riemer and Jones 2014), with cyclones to the east of the tip recurving relative to the trough and gaining latitude. These cyclones often undergo substantial extratropical reintensification, in contrast to cyclones which do not recurve relative to the trough.

The NoEurope PTCs also recurve in the presence of an upstream trough but do not approach the trough as closely as the Europe PTCs. They also remain in a region of weaker geopotential height gradients and lower Eady growth rates than the Europe PTCs. The trough remains poleward of the cyclone, and weaker TC–trough interaction occurs compared to the Europe PTCs. In the NoEurope composite, the cyclones are not steered poleward, and do not interact with the jet streak. This is consistent with the northeast pattern described in Harr et al. (2000), in which the cyclones do not undergo substantial extratropical reintensification. It is described therein that the strong zonal flow between the subtropical high and the midlatitudes prevents a coupling with a midlatitude baroclinic zone. The Europe PTCs exhibit similar behavior in terms of jet interaction as the TC-decelerating trough composite in Riboldi et al. (2019), in which the PTC interacts with and subsequently crosses the jet streak situated on the eastern flank of the upstream trough in the 2 days following ET completion. Conversely, the PTCs comprising the TC-accelerating trough composite of Riboldi et al. (2019) do not interact with and cross the jet streak, similar to the NoEurope PTCs presented in Fig. 6. However, differences in meridional deflection of the jet and extent of downstream ridge building are also found between the accelerating and decelerating trough composites, which are not clearly visible in Fig. 6.

Hart et al. (2006) found that cyclones which reintensify post-ET are associated with a negatively tilted trough (oriented from northwest to southeast), whereas the post-ET weakening storms are associated with a positively tilted trough. The troughs in the PTC-decelerating trough composite of Riboldi et al. (2019), which subsequently cross the midlatitude jet streak, also appear to have a negative tilt. However, Fig. 6 of our analysis shows that the tilt of the trough may not be

important for the post-ET reintensification of PTCs, as the troughs in the Europe and NoEurope composites have a very similar orientation. Further work would be necessary to confirm this. In Hart et al. (2006), it is hypothesized that the negative tilt of the upstream trough permits the cyclone a closer approach to the trough, leading to a contraction and intensification of the eddy potential vorticity flux. Recent work suggests that the negative tilt may be the result of strong TC–trough interaction, rather than a predictor of future PTC intensity (Sarro and Evans 2022).

In addition to more directly interacting with the jet, the Europe PTCs are associated with a jet which is significantly more intense than the jet associated with the NoEurope PTCs. At each time step shown in Fig. 6, the maximum jet speed within $10°$ of the Europe PTCs is significantly (~7 m s^{-1}) higher than for the NoEurope PTCs. Maximum 300-hPa winds in the composite mean jet streak are approximately 10 m s^{-1} higher for the Europe PTCs than the NoEurope PTCs (Fig. 7). This may indicate that Europe PTCs interact with a more baroclinic midlatitude environment (as suggested by the higher Eady growth rates). However, the difference in jet speeds could also result from local jet streak amplification resulting from negative potential vorticity advection from the divergent outflow of the TC (Riboldi et al. 2019; Keller et al. 2019), which may also be expected given the greater PV advection by the irrotational wind associated with Europe PTCs at 24 h prior to ET completion.

The difference in baroclinicity surrounding the Europe and NoEurope PTCs motivates an investigation into the seasonality of the two composites. The fraction of PTCs which reach Europe increases throughout the hurricane season, from ~15% for TCs completing ET in July to 50% for TCs completing ET in November (Fig. S1).

d. The association between extratropical reintensification and Europe-impact likelihood

We have shown that PTCs that impact Europe tend to (i) transition into a more favorable environment for reintensification, and (ii) develop characteristics associated with a reintensifying cyclone. In this section we test the hypothesis that PTCs that reintensify after ET are more likely to reach Europe. This is achieved by separating the Europe and NoEurope PTCs which reintensify from those that do not. The proportion of PTCs in both composites that reintensify, along with the mean reintensification in each composite, can then be investigated. We then recomposite the reintensifying cyclones about the point of reintensification, to investigate the features of the midlatitude circulation that are associated with reintensification.

Figure 8 shows the composite life cycle of the Europe PTCs (red) and NoEurope PTCs (blue), based on whether they reintensify in the midlatitudes or not. PTCs are designated as reintensifying if at some point post-ET, they undergo an increase in 850-hPa T63 spectrally filtered relative vorticity (the field used for cyclone tracking) of 3×10^{-5} s^{-1} or larger, where the 6-hourly T63 relative vorticity fields have been smoothed using a 5-point running mean to remove
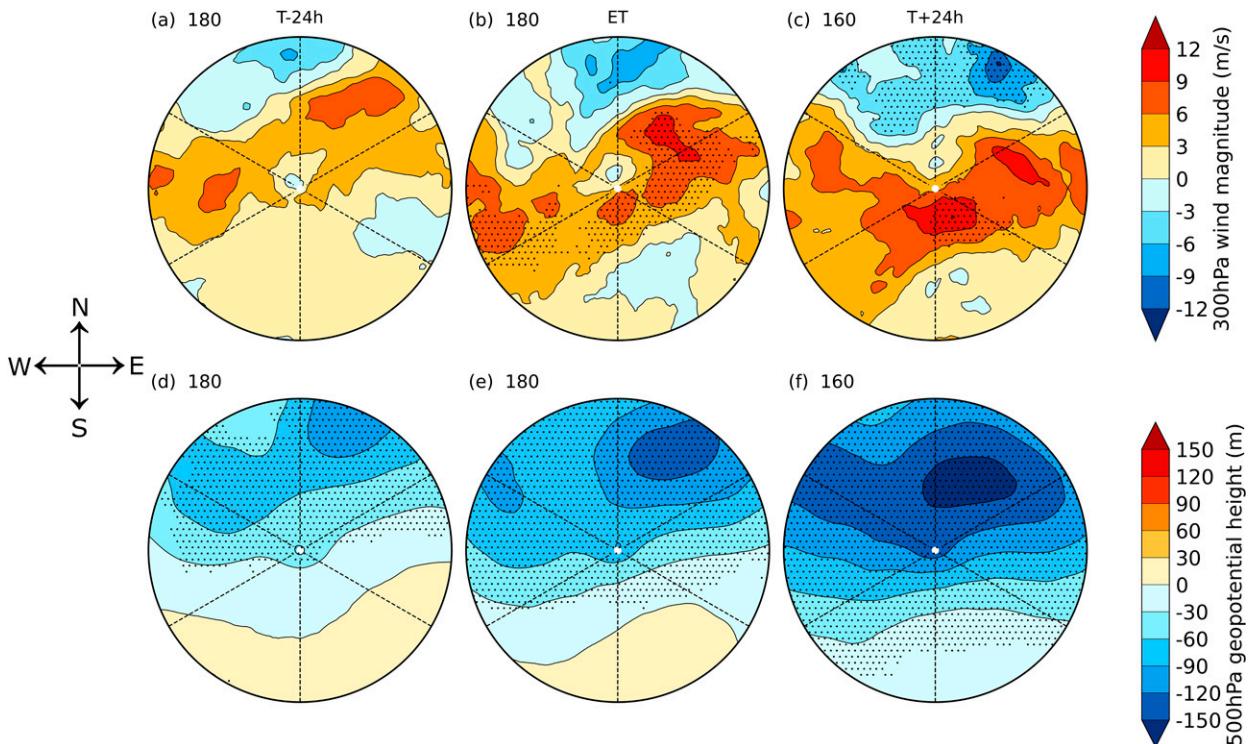
FIG. 7. Difference (Europe minus NoEurope) of the (top) composite mean (20° cap) cyclone-relative 300-hPa wind magnitude and (bottom) 500-hPa geopotential height at (a),(d) 24 h prior to ET completion; (b),(e) ET completion; and (c),(f) 24-h post-ET completion. Cyclones are not aligned based on their direction of travel. Stippling represents areas in which the composite mean wind magnitudes are significantly different (95%). Sample size is shown in the upper left of each panel.

high-frequency variability in intensity. A five-time-step running mean is chosen as it is long enough to sufficiently smooth out high-frequency variability within the data without significantly dampening robust changes in vorticity due to reintensification. Overlaid crosses are the time steps at which there is a significant (95% level) difference between the mean 850-hPa T63 relative vorticity for the Europe/NoEurope reintensifiers, and the Europe/NoEurope weakeners.

The Europe PTCs have a much higher T63 relative vorticity at ET completion than the NoEurope PTCs. This is particularly clear for the Europe weakening composite. This indicates that the strength of the TC may be important in modulating the likelihood that a PTC will reach Europe. The NoEurope PTCs which reintensify appear to intensify more than the Europe intensifiers; however, this is due to a large spread in the time relative to ET at which the cyclones undergo reintensification. On average, the reintensification amounts are 8.8 and $6.8 \times 10^{-5} \text{ s}^{-1}$ for the Europe and NoEurope reintensifiers, respectively, although this difference is not statistically significant ($p = 0.12$). A larger proportion of the Europe PTCs are identified as reintensifying (42%) compared to NoEurope PTCs (21%). This highlights the importance of both TC intensity and the midlatitude environment into which the TC transitions in determining whether the PTC will reach Europe.

Figure 9 shows the storm-centered composites for the Europe reintensifiers and the NoEurope reintensifiers. Instead of centering the composites about ET completion, we now center them about the onset of reintensification (left), time of max reintensification rate (middle) and maximum post-ET intensity (right). The onset of reintensification is the time step after ET completion at which the T63 relative vorticity begins to increase. The time of maximum intensification rate is the time step at which the max 6-hourly T63 relative vorticity increase occurs between reintensification onset and maximum intensity. Max post-ET intensity is the time step of the maximum T63 relative vorticity post-ET.

The PTCs in both composites begin reintensification as they begin to interact with the right entrance of the jet streak. They reach their maximum rate of reintensification when superposed with the jet maximum and attain their maximum intensity when they have exited the jet and are situated by the left exit region. The right entrance and left exit regions of the jet are regions of enhanced upper-level divergence (Klein et al. 2002), which may act to aid the reintensification process. The Europe reintensifiers cross a stronger composite mean jet than the NoEurope reintensifiers and undergo more intensification.

e. Relative importance of TC intensity and reintensification

The analyses presented in sections 3b and 3d suggest that there is a strong association between the likelihood that a PTC will impact Europe and 1) the intensity of the TC, both at the lifetime maximum intensity of the storm and as it
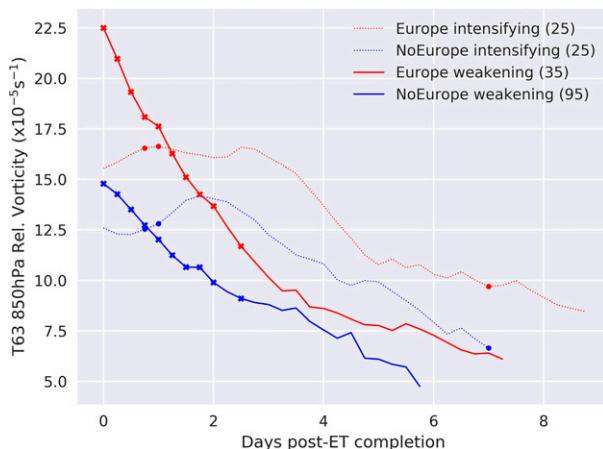
FIG. 8. Composite life cycle of the 850-hPa relative vorticity, spectrally filtered to a T63 spectral resolution, for the Europe (red) and NoEurope PTCs (blue) centered on ET completion and separated based on whether they reintensify (dashed) or weaken (solid) post-ET. Data from ERA5 are used, and all TCs that complete ET in ERA5 (180) are included in the composite. Crosses and dots represent the time steps at which the difference in the composite means is significant to 95% using a Kolmogorov–Smirnov test [comparing Europe reintensifiers with NoEurope reintensifiers (dots), and Europe weakeners with NoEurope weakeners (crosses)]. The sample size in each composite is shown in the legend.

begins ET, and 2) whether the cyclone reintensifies after ET. In this section, we investigate the association between each factor and the likelihood that a cyclone will impact Europe in more detail and investigate the relative importance of both factors.

Figure 10 shows the conditional probability that a PTC will impact Europe based on its intensity at TC lifetime maximum intensity, intensity at ET onset, and the amount of reintensification that the cyclone undergoes post-ET. TC lifetime maximum intensity and reintensification are chosen because there are significant differences in these metrics when comparing the Europe and NoEurope PTCs (Figs. 2 and 8, respectively). TC lifetime maximum intensity is defined as the maximum wind speed associated with a TC in HURDAT2 up to the point of ET completion, as determined using the ERA5 cyclone phase space analysis. Intensity at ET onset is investigated because it better represents the intensity that the TC has when it begins interacting with the midlatitude environment than TC lifetime maximum intensity. However, we have fewer data available for this metric (see columns 2 and 3 of Table 1 for sample sizes of TC lifetime maximum intensity and ET onset intensity, respectively). As a result, the number of storms going into Fig. 10b is smaller than Figs. 10a and 10c. Bin edges used for Figs. 10a and 10b are (from left to right) <20th percentile, 20th–40th percentile, 40th–60th percentile, 60th–80th percentile, and >80th percentile of the combined distribution. For reintensification (Fig. 10c), the bin percentiles are <40th percentile, 40th–55th percentile, 55th–70th percentile, 70th–85th percentile, and >85th percentile. It was necessary to choose different percentiles to bin storms based

on reintensification because more than 20% of storms do not reintensify at all. The combined distribution is comprised of all the Europe and NoEurope PTCs, and the percentile bin edges are used to ensure a consistent sample size across bins.

There is a clear increasing trend in Figs. 10a–c. For TC lifetime maximum intensity, only ~22% of the weakest PTCs impact Europe, compared to almost 50% for the strongest 20%. Only 10% of the weakest PTCs at ET onset impact Europe, compared to over 50% for the strongest 20%. For reintensification there is also a trend. Approximately 20% of storms which do not reintensify at all (bin 1) make it to Europe, compared to ~60% for the storms which undergo the most reintensification. Figure 10 highlights that both the midlatitude environment, which largely facilitates reintensification, and TC intensity, are strongly associated with Europe-impact likelihood.

Figure 10d shows the relationship between the TC lifetime maximum intensity and the reintensification post-ET. The correlation between TC lifetime maximum intensity and reintensification post-ET is weak but significant, with a Pearson's correlation coefficient of −0.2. The lack of a strong association between reintensification and TC intensity combined with Figs. 10a and 10c, which show that stronger TCs (at TC lifetime maximum intensity) and storms which reintensify are more likely to impact Europe, indicate that both factors are associated with whether a PTC will impact Europe. The lack of association between reintensification and TC intensity also suggests that while both factors are important in modulating the likelihood that a PTC will reach Europe, they may not both be important for the same PTC. This suggests that there may be two pathways through which a PTC can reach Europe: a strong TC that gradually weakens on approach, or a TC (which may not necessarily be a strong TC) that undergoes substantial reintensification in a favorable midlatitude environment after ET. Furthermore, the lack of association between TC intensity and reintensification is consistent with previous studies which suggest that TC intensity is not a primary factor determining whether a favorable phase-locked configuration will exist between the transitioning TC and the upstream trough (Archambault et al. 2013; Brannan and Chagnon 2020).

Table 4 shows a joint contingency table to further investigate the association that TC intensity and reintensification have with PTCs reaching Europe, with the Odds ratios displayed in Fig. 11. TC lifetime maximum intensity and reintensification have odds ratios of 2.38 and 2.71, respectively. In both cases, the lower bound 95% confidence interval (brackets, Fig. 11) are greater than 1, indicating a significant association between TC lifetime maximum intensity, reintensification, and whether a PTC reaches Europe. Odds ratios for reintensification conditioned on TC lifetime maximum intensity, Odds(Europe$|_{R,\mathrm{MH}}$)/Odds(Europe$|_{w,\mathrm{MH}}$) and Odds(Europe$|_{R,\mathrm{NON-MH}}$)/Odds(Europe$|_{w,\mathrm{NON-MH}}$), are 3.1 (nonsignificant) and 3.45 (significant), respectively. Similarly, odds ratios for TC lifetime maximum intensity conditioned on reintensification, Odds(Europe$|_{\mathrm{MH}_R}$)/Odds(Europe$|_{\mathrm{NON-MH}_R}$) and Odds(Europe$|_{\mathrm{MH,W}}$)/Odds(Europe$|_{\mathrm{NON-MH,W}}$) are 2.47 (nonsignificant) and 2.75 (significant). When only considering
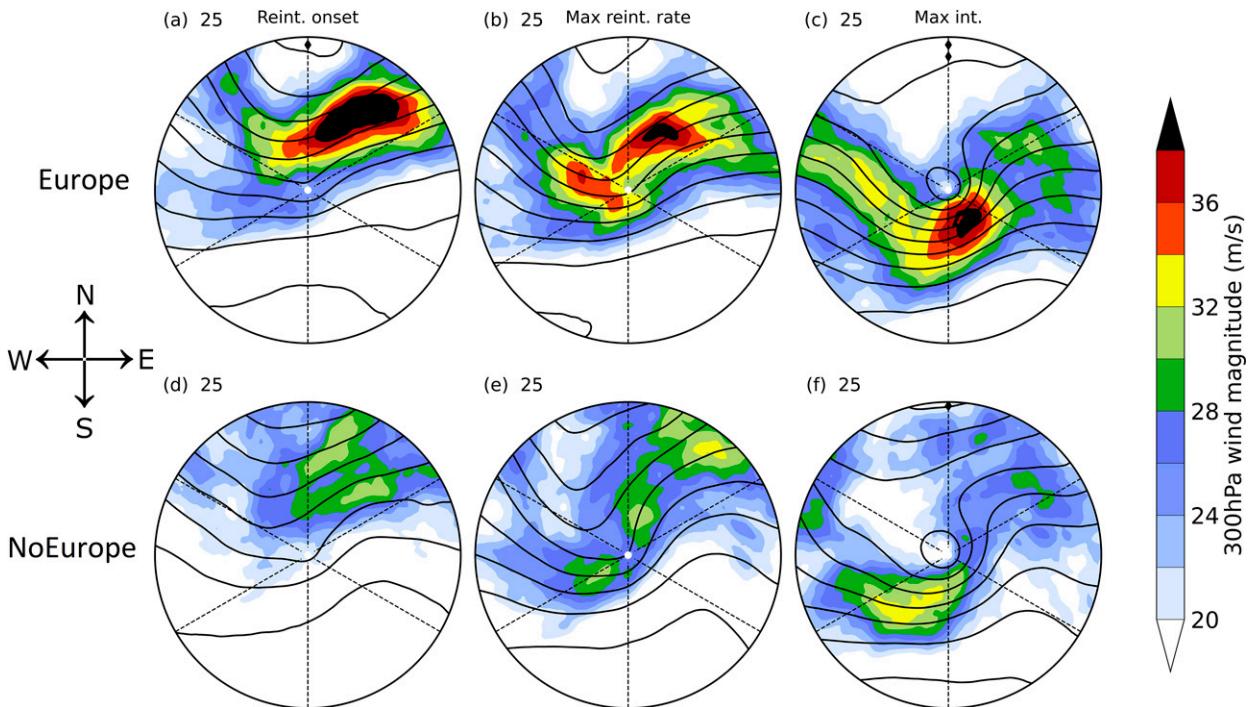
FIG. 9. Storm-centered composites (20° cap) showing the 300-hPa wind magnitude (filled contours) and 500-hPa geopotential height (black open contours) for (a)–(c) the Europe PTCs that reintensify and (d)–(f) the NoEurope PTCs that reintensify. Composites are centered about the point of (left) post-ET reintensification onset, (center) post-ET max intensification rate, and (right) post-ET maximum intensity. Cyclones are not aligned based on their direction of travel. Sample size is shown in the upper left of each panel.

weak TCs the role of reintensification appears larger, and when only considering weakening storms post-ET the role of TC lifetime maximum intensity is larger (higher odds ratios). This shows that PTCs usually need at least one of these factors in order to reach Europe; however, having both factors does not further increase the odds of reaching Europe significantly compared to just one factor (95% confidence interval includes 1).

A small fraction of NoEurope PTCs were major hurricanes and reintensified post-ET (4/120). Of these four cyclones, three made landfall across the continental United States and traveled northeastward across northeastern Canada, undergoing brief reintensification before dissipating. The fourth PTC traveled poleward toward Greenland after ET. Similarly, there are some Europe PTCs that neither reintensify nor were major hurricanes (15/60). This subgroup of Europe PTCs recurves farther east in the basin, with 10/15 completing ET east of 30°W (Fig. S2). When considering all PTCs, there is also a significant association between the longitude of ET completion and the odds of reaching Europe (Fig. 11) when using a threshold of 70°W.

4. Summary and conclusions

PTCs can bring severe weather to Europe in terms of extreme precipitation, high winds, and large waves. These PTCs have been associated with national record wind gusts across Ireland as well as large economic losses across Europe.

However, many PTCs never make it to Europe at all. In this study, we try to understand the factors which determine whether a PTC will impact Europe. This is achieved by identifying the observed PTCs in the ERA5 reanalysis using a feature tracking scheme, allowing us to undertake detailed analysis of the post-tropical stage of these storms.

Using a composite analysis, we show that PTCs which impact Europe are much more likely to undergo extratropical reintensification than PTCs which do not impact Europe (NoEurope). By quantifying the area-averaged negative potential vorticity advection by the irrotational wind in the vicinity of the PTCs (Archambault et al. 2013), the Europe PTCs are shown to interact more strongly with an upstream trough at a much closer distance to the storm center during extratropical transition (ET) than the NoEurope PTCs. This is consistent with previous studies which highlight the importance of TC–trough interactions for PTC reintensification and downstream flow amplification (Hart et al. 2006; Keller et al. 2019; Riboldi et al. 2019). During ET, the baroclinicity, characterized by the Eady growth rate, is significantly higher in the vicinity of Europe PTCs than NoEurope PTCs. Baroclinicity generally increases throughout hurricane season, and TCs completing ET in October and November are more likely to reach Europe than those completing ET earlier in the season. The Europe PTCs travel on a more poleward trajectory, allowing them to interact with a midlatitude jet streak. It is at this point that many of the storms in the Europe PTCs undergo reintensification. The NoEurope PTCs travel
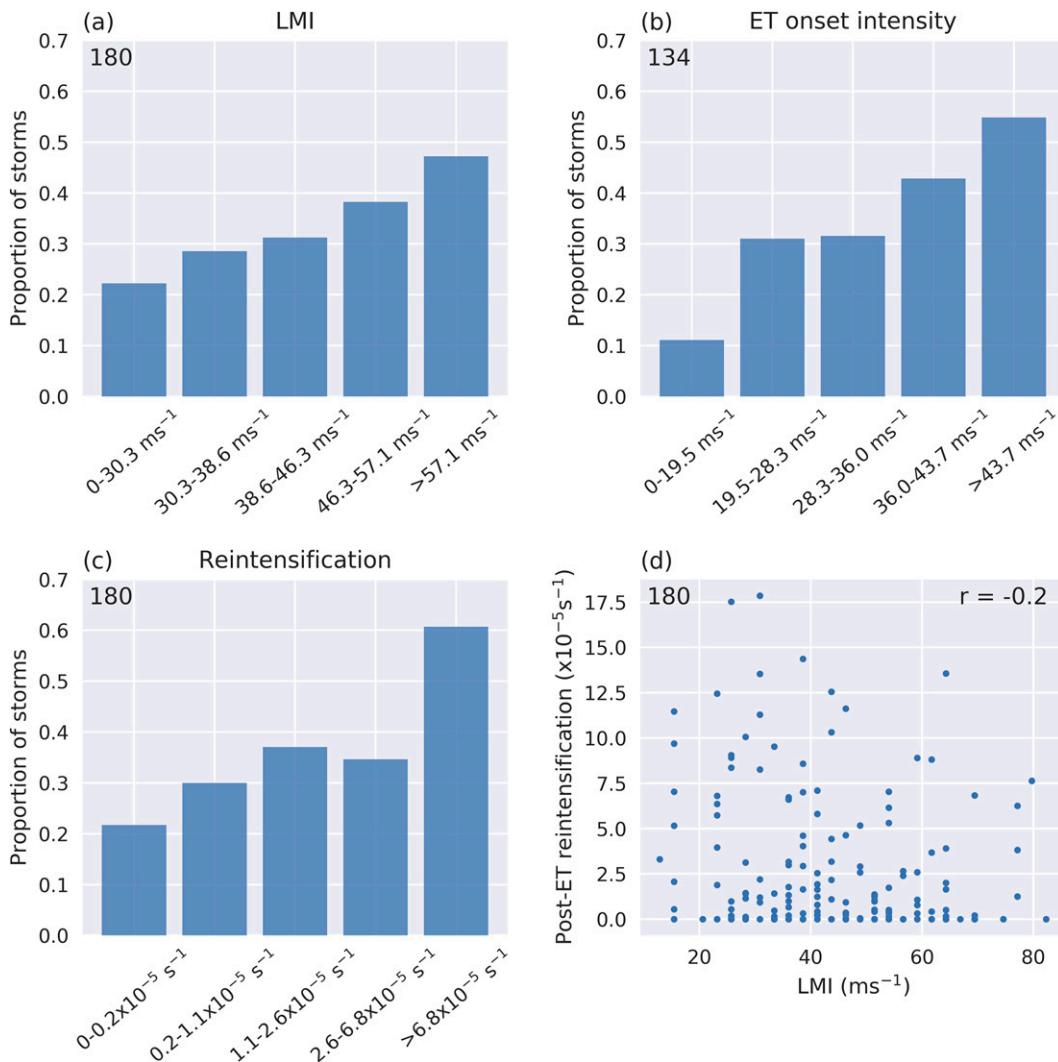
FIG. 10. Conditional probability that a PTC will impact Europe based on (a) the TC lifetime maximum intensity, (b) intensity at ET onset, and (c) T63 relative vorticity increase post-ET. (d) A scatterplot of TC lifetime maximum intensity and T63 relative vorticity increase post-ET for all Europe and NoEurope PTCs. Sample size is shown in the upper left of each panel.

less poleward after ET, and the composite mean does not directly interact with a midlatitude jet streak. The NoEurope PTCs are also less likely to reintensify.

The Europe PTCs also have a substantially higher intensity in their TC phase, both at their lifetime maximum intensity and as they begin ET as they enter the midlatitudes. Contingency table analysis suggests that both TC intensity and whether reintensification occurs post-ET modulate the likelihood that the storm will impact Europe, although these factors may not be important for the same PTC. Our results indicate that the mid

TABLE 4. Joint contingency table for PTCs separated based on whether they reintensify of weaken post-ET, were a major hurricane at their lifetime maximum intensity, and whether they impact Europe.

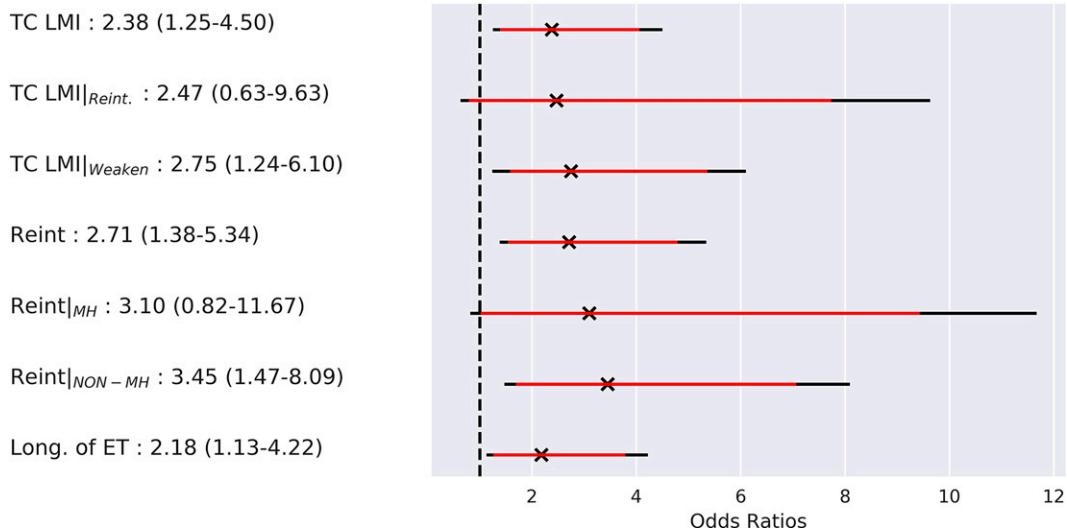|	TC lifetime max intensity ≥ 50 m s^{-1} (major hurricane)			TC lifetime max intensity < 50 m s^{-1} (non-major hurricane)		
	Europe	NoEurope	Total	Europe	NoEurope	Total
Reintensify post-ET	8	4	12	17	21	38
Weaken post-ET	20	31	51	15	64	79
Total	28	35	63	32	85	117

FIG. 11. Odds ratios (black crosses) and associated 95% (black horizontal lines) and 90% (red horizontal lines) confidence intervals for TC intensity, reintensification, and longitude of ET completion. Vertical dashed black line indicates an odds ratio of 1. Numbers and parentheses to the left of the panel show the odds ratios and the associated 95% confidence interval.

latitude environment into which the TCs recurve and the strength of the TCs are key to understanding why some PTCs impact Europe. The importance of TC intensity is consistent with previous studies, which suggest that PTCs may retain some "memory" of the tropical phase of their life cycle during, and potentially after, ET (Datt et al. 2022). All results presented in this paper have been verified using a second reanalysis, MERRA2 (Gelaro et al. 2017; Molod et al. 2015), and results very similar to ERA5 (not shown).

This paper has focused on the characteristics of the cyclones themselves and the surrounding environment. An investigation of the larger scale atmospheric circulation, such as the phase of the NAO, may also provide some insight into why some PTCs reach Europe. It could be hypothesized that positive NAO conditions may lead to greater longevity, faster translation, or a higher likelihood of reintensification, and therefore may have implications for the probability that a PTC will reach Europe. This will be investigated in future work.

In the context of climate change, our results highlight the challenges of projecting PTC impacts over Europe in a future climate, as has been highlighted for ET more generally in the North Atlantic basin (Zarzycki et al. 2017). In this study, we have shown that TC intensity and post-ET reintensification are key metrics of model fidelity. Some climate model projections indicate a poleward shift in the jet (Harvey et al. 2020), possibly signaling less opportunity for PTCs to interact with the jet, leading to less extratropical reintensification. However, SSTs are projected to warm, and TC lifetime maximum intensity may increase as a result. Previous studies suggest that this may already be occurring (Kossin et al. 2020). If the change in TC intensity outweighs any potential poleward shift in the jet, then in the future a larger proportion of PTCs may reach Europe.

REFERENCES

Agusti-Panareda, A., C. D. Thorncroft, G. C. Craig, and S. L. Gray, 2004: The extratropical transition of Hurricane Irene (1999): A potential-vorticity perspective. *Quart. J. Roy. Meteor. Soc.*, **130**, 1047–1074, https://doi.org/10.1256/qj.02.140.

Anwender, D., P. A. Harr, and S. C. Jones, 2008: Predictability associated with the downstream impacts of the extratropical transition of tropical cyclones: Case studies. *Mon. Wea. Rev.*, **136**, 3226–3247, https://doi.org/10.1175/2008MWR2249.1.

Archambault, H. M., L. F. Bosart, D. Keyser, and J. M. Cordeira, 2013: A climatological analysis of the extratropical flow

response to recurring western North Pacific tropical cyclones. *Mon. Wea. Rev.*, **141**, 2325–2346, https://doi.org/10.1175/MWR-D-12-00257.1.

——, D. Keyser, L. F. Bosart, C. A. Davis, and J. M. Cordeira, 2015: A composite perspective of the extratropical flow response to recurring western North Pacific tropical cyclones. *Mon. Wea. Rev.*, **143**, 1122–1141, https://doi.org/10.1175/MWR-D-14-00270.1.

Baatsen, M., R. J. Haarsma, A. J. Van Delden, and H. de Vries, 2015: Severe autumn storms in future Western Europe with a warmer Atlantic Ocean. *Climate Dyn.*, **45**, 949–964, https://doi.org/10.1007/s00382-014-2329-8.

Baker, A. J., K. I. Hodges, R. K. H. Schiemann, and P. L. Vidale, 2021: Historical variability and lifecycles of North Atlantic midlatitude cyclones originating in the tropics. *J. Geophys. Res. Atmos.*, **126**, e2020JD033924, https://doi.org/10.1029/2020JD033924.

——, and Coauthors, 2022: Extratropical transition of tropical cyclones in a multiresolution ensemble of atmosphere-only and fully coupled global climate models. *J. Climate*, **35**, 5283–5306, https://doi.org/10.1175/JCLI-D-21-0801.1.

Bengtsson, L., K. I. Hodges, M. Esch, N. Keenlyside, L. Kornblueh, J.-J. Luo, and T. Yamagata, 2007: How may tropical cyclones change in a warmer climate? *Tellus*, **59A**, 539–561, https://doi.org/10.1111/j.1600-0870.2007.00251.x.

Bieli, M., S. J. Camargo, A. H. Sobel, J. L. Evans, and T. Hall, 2019: A global climatology of extratropical transition. Part I: Characteristics across basins. *J. Climate*, **32**, 3557–3582, https://doi.org/10.1175/JCLI-D-17-0518.1.

Brannan, A. L., and J. M. Chagnon, 2020: A climatology of the extratropical flow response to recurving Atlantic tropical cyclones. *Mon. Wea. Rev.*, **148**, 541–558, https://doi.org/10.1175/MWR-D-19-0216.1.

Catto, J. L., L. C. Shaffrey, and K. I. Hodges, 2010: Can climate models capture the structure of extratropical cyclones? *J. Climate*, **23**, 1621–1635, https://doi.org/10.1175/2009JCLI3318.1.

Dacre, H. F., M. K. Hawcroft, M. A. Stringer, and K. I. Hodges, 2012: An extratropical cyclone atlas a tool for illustrating cyclone structure and evolution characteristics. *Bull. Amer. Meteor. Soc.*, **93**, 1497–1502, https://doi.org/10.1175/BAMS-D-11-00164.1.

Datt, I., S. J. Camargo, A. H. Sobel, R. McTaggart-Cowan, and Z. Wang, 2022: An investigation of tropical cyclone development pathways as an indicator of extratropical transition. *J. Meteor. Soc. Japan*, **100**, 707–724, https://doi.org/10.2151/jmsj.2022-037.

Davis, C. A., 2018: Resolving tropical cyclone intensity in models. *Geophys. Res. Lett.*, **45**, 2082–2087, https://doi.org/10.1002/2017GL076966.

Dekker, M. M., R. J. Haarsma, H. de Vries, M. Baatsen, and A. J. va. Delden, 2018: Characteristics and development of European cyclones with tropical origin in reanalysis data. *Climate Dyn.*, **50**, 445–455, https://doi.org/10.1007/s00382-017-3619-8.

Delgado, S., C. W. Landsea, and H. Willoughby, 2018: Reanalysis of the 1954–63 Atlantic hurricane seasons. *J. Climate*, **31**, 4177–4192, https://doi.org/10.1175/JCLI-D-15-0537.1.

Evans, C., and Coauthors, 2017: The extratropical transition of tropical cyclones. Part I: Cyclone evolution and direct impacts. *Mon. Wea. Rev.*, **145**, 4317–4344, https://doi.org/10.1175/MWR-D-17-0027.1.

Gelaro, R., and Coauthors, 2017: The Modern-Era Retrospective Analysis for Research and Applications, version 2 (MERRA-2).

J. Climate, **30**, 5419–5454, https://doi.org/10.1175/JCLI-D-16-0758.1.

Graham, E., and D. Smart, 2021: 'Hurricane' Debbie—60 years on: A fresh analysis. *Weather*, **76**, 284–292, https://doi.org/10.1002/wea.4051.

Grams, C. M., and S. R. Blumer, 2015: European high-impact weather caused by the downstream response to the extratropical transition of North Atlantic Hurricane Katia (2011). *Geophys. Res. Lett.*, **42**, 8738–8748, https://doi.org/10.1002/2015GL066253.

——, S. C. Jones, C. A. Davis, P. A. Harr, and M. Weissmann, 2013a: The impact of Typhoon Jangmi (2008) on the midlatitude flow. Part I: Upper-level ridgebuilding and modification of the jet. *Quart. J. Roy. Meteor. Soc.*, **139**, 2148–2164, https://doi.org/10.1002/qj.2091.

——, ——, and ——, 2013b: The impact of Typhoon Jangmi (2008) on the midlatitude flow. Part II: Downstream evolution. *Quart. J. Roy. Meteor. Soc.*, **139**, 2165–2180, https://doi.org/10.1002/qj.2119.

Haarsma, R. J., and Coauthors, 2013: More hurricanes to hit Western Europe due to global warming. *Geophys. Res. Lett.*, **40**, 1783–1788, https://doi.org/10.1002/grl.50360.

Hagen, A. B., D. Strahan-Sakoskie, and C. Luckett, 2012: A reanalysis of the 1944–53 Atlantic hurricane seasons—The first decade of aircraft reconnaissance. *J. Climate*, **25**, 4441–4460, https://doi.org/10.1175/JCLI-D-11-00419.1.

Harr, P. A., R. L. Elsberry, and T. F. Hogan, 2000: Extratropical transition of tropical cyclones over the western North Pacific Part II: The impact of midlatitude circulation characteristics. *Mon. Wea. Rev.*, **128**, 2634–2653, https://doi.org/10.1175/1520-0493(2000)128<2634:ETOTCO>2.0.CO;2.

Hart, R. E., 2003: A cyclone phase space derived from thermal wind and thermal asymmetry. *Mon. Wea. Rev.*, **131**, 585–616, https://doi.org/10.1175/1520-0493(2003)131<0585:ACPSDF>2.0.CO;2.

——, and J. L. Evans, 2001: A climatology of the extratropical transition of Atlantic tropical cyclones. *J. Climate*, **14**, 546–564, https://doi.org/10.1175/1520-0442(2001)014<0546:ACOTET>2.0.CO;2.

——, ——, and C. Evans, 2006: Synoptic composites of the extratropical transition life cycle of North Atlantic tropical cyclones: Factors determining posttransition evolution. *Mon. Wea. Rev.*, **134**, 553–578, https://doi.org/10.1175/MWR3082.1.

Harvey, B. J., P. Cook, L. C. Shaffrey, and R. Schiemann, 2020: The response of the Northern Hemisphere storm tracks and jet streams to climate change in the CMIP3, CMIP5, and CMIP6 climate models. *J. Geophys. Res. Atmos.*, **125**, e2020JD032701, https://doi.org/10.1029/2020JD032701.

Hersbach, H., and Coauthors, 2020: The ERA5 global reanalysis. *Quart. J. Roy. Meteor. Soc.*, **146**, 1999–2049, https://doi.org/10.1002/qj.3803.

Hodges, K., A. Cobb, and P. L. Vidale, 2017: How well are tropical cyclones represented in reanalysis datasets? *J. Climate*, **30**, 5243–5264, https://doi.org/10.1175/JCLI-D-16-0557.1.

Hoskins, B. J., and P. J. Valdes, 1990: On the existence of storm-tracks. *J. Atmos. Sci.*, **47**, 1854–1864, https://doi.org/10.1175/1520-0469(1990)047<1854:OTEOST>2.0.CO;2.

Jones, S. C., and Coauthors, 2003: The extratropical transition of tropical cyclones: Forecast challenges, current understanding, and future directions. *Wea. Forecasting*, **18**, 1052–1092, https://doi.org/10.1175/1520-0434(2003)018<1052:TETOTC>2.0.CO;2.

Keller, J. H., 2017: Amplification of the downstream wave train during extratropical transition: Sensitivity studies. *Mon. Wea. Rev.*, **145**, 1529–1548, https://doi.org/10.1175/MWR-D-16-0193.1.

——, and Coauthors, 2019: The extratropical transition of tropical cyclones. Part II: Interaction with the midlatitude flow, downstream impacts, and implications for predictability. *Mon. Wea. Rev.*, **147**, 1077–1106, https://doi.org/10.1175/MWR-D-17-0329.1.

Klein, P. M., P. A. Harr, and R. L. Elsberry, 2000: Extratropical transition of western North Pacific tropical cyclones: An overview and conceptual model of the transformation stage. *Wea. Forecasting*, **15**, 373–395, https://doi.org/10.1175/1520-0434(2000)015<0373:ETOWNP>2.0.CO;2.

——, ——, and ——, 2002: Extratropical transition of western North Pacific tropical cyclones: Midlatitude and tropical cyclone contributions to reintensification. *Mon. Wea. Rev.*, **130**, 2240–2259, https://doi.org/10.1175/1520-0493(2002)130<2240:ETOWNP>2.0.CO;2.

Kossin, J. P., K. R. Knapp, T. L. Olander, and C. S. Velden, 2020: Global increase in major tropical cyclone exceedance probability over the past four decades. *Proc. Natl. Acad. Sci. USA*, **117**, 11 975–11 980, https://doi.org/10.1073/pnas.1920849117.

Landsea, C. W., 1993: A climatology of intense (or major) Atlantic hurricanes. *Mon. Wea. Rev.*, **121**, 1703–1713, https://doi.org/10.1175/1520-0493(1993)121<1703:ACOIMA>2.0.CO;2.

——, and J. L. Franklin, 2013: Atlantic hurricane database uncertainty and presentation of a new database format. *Mon. Wea. Rev.*, **141**, 3576–3592, https://doi.org/10.1175/MWR-D-12-00254.1.

Laurila, T. K., V. A. Sinclair, and H. Gregow, 2020: The extratropical transition of Hurricane Debby (1982) and the subsequent development of an intense windstorm over Finland. *Mon. Wea. Rev.*, **148**, 377–401, https://doi.org/10.1175/MWR-D-19-0035.1.

Liu, M., G. A. Vecchi, J. A. Smith, and H. Murakami, 2017: The present-day simulation and twenty-first-century projection of the climatology of extratropical transition in the North Atlantic. *J. Climate*, **30**, 2739–2756, https://doi.org/10.1175/JCLI-D-16-0352.1.

McTaggart-Cowan, R., J. R. Gyakum, and M. K. Yau, 2001: Sensitivity testing of extratropical transitions using potential vorticity inversions to modify initial conditions: Hurricane Earl case study. *Mon. Wea. Rev.*, **129**, 1617–1636, https://doi.org/10.1175/1520-0493(2001)129<1617:STOETU>2.0.CO;2.

——, ——, and ——, 2003: The influence of the downstream state on extratropical transition: Hurricane Earl (1998) case study. *Mon. Wea. Rev.*, **131**, 1910–1929, https://doi.org/10.1175/2589.1.

——, ——, and ——, 2004: The impact of tropical remnants on extratropical cyclogenesis: Case study of Hurricanes Danielle and Earl (1998). *Mon. Wea. Rev.*, **132**, 1933–1951, https://doi.org/10.1175/1520-0493(2004)132<1933:TIOTRO>2.0.CO;2.

Molod, A., L. Takacs, M. Suarez, and J. Bacmeister, 2015: Development of the GEOS-5 atmospheric general circulation model: Evolution from MERRA to MERRA2. *Geosci. Model Dev.*, **8**, 1339–1356, https://doi.org/10.5194/gmd-8-1339-2015.

Pantillon, F. P., J.-P. Chaboureau, P. J. Mascart, and C. Lac, 2013: Predictability of a Mediterranean tropical-like storm downstream of the extratropical transition of Hurricane Helene (2006). *Mon. Wea. Rev.*, **141**, 1943–1962, https://doi.org/10.1175/MWR-D-12-00164.1.

Pantillon, F., J.-P. Chaboureau, and E. Richard, 2015: Remote impact of North Atlantic hurricanes on the Mediterranean during episodes of intense rainfall in autumn 2012. *Quart. J.*

Roy. Meteor. Soc., **141**, 967–978, https://doi.org/10.1002/qj.2419.

——, ——, and ——, 2016: Vortex–vortex interaction between Hurricane Nadine (2012) and an Atlantic cut-off dropping the predictability over the Mediterranean. *Quart. J. Roy. Meteor. Soc.*, **142**, 419–432, https://doi.org/10.1002/qj.2635.

Pohorsky, R., M. Röthlisberger, C. M. Grams, J. Riboldi, and O. Martius, 2019: The climatological impact of recurving North Atlantic tropical cyclones on downstream extreme precipitation events. *Mon. Wea. Rev.*, **147**, 1513–1532, https://doi.org/10.1175/MWR-D-18-0195.1.

Quinting, J. F., and S. C. Jones, 2016: On the impact of tropical cyclones on Rossby wave packets: A climatological perspective. *Mon. Wea. Rev.*, **144**, 2021–2048, https://doi.org/10.1175/MWR-D-14-00298.1.

Rantanen, M., J. Räisänen, V. A. Sinclair, J. Lento, and H. Järvinen, 2020: The extratropical transition of Hurricane Ophelia (2017) as diagnosed with a generalized omega equation and vorticity equation. *Tellus*, **72A**, 1721215, https://doi.org/10.1080/16000870.2020.1721215.

Riboldi, J., C. M. Grams, M. Riemer, and H. M. Archambault, 2019: A phase locking perspective on Rossby wave amplification and atmospheric blocking downstream of recurving western North Pacific tropical cyclones. *Mon. Wea. Rev.*, **147**, 567–589, https://doi.org/10.1175/MWR-D-18-0271.1.

Riemer, M., and S. C. Jones, 2010: The downstream impact of tropical cyclones on a developing baroclinic wave in idealized scenarios of extratropical transition. *Quart. J. Roy. Meteor. Soc.*, **136**, 617–637, https://doi.org/10.1002/qj.605.

——, and ——, 2014: Interaction of a tropical cyclone with a high-amplitude, midlatitude wave pattern: Waviness analysis, trough deformation and track bifurcation. *Quart. J. Roy. Meteor. Soc.*, **140**, 1362–1376, https://doi.org/10.1002/qj.2221.

——, ——, and C. A. Davis, 2008: The impact of extratropical transition on the downstream flow: An idealized modelling study with a straight jet. *Quart. J. Roy. Meteor. Soc.*, **134**, 69–91, https://doi.org/10.1002/qj.189.

Russell, J. O., A. Aiyyer, J. D. White, and W. Hannah, 2017: Revisiting the connection between African easterly waves and Atlantic tropical cyclogenesis. *Geophys. Res. Lett.*, **44**, 587–595, https://doi.org/10.1002/2016GL071236.

Sainsbury, E. M., R. K. H. Schiemann, K. I. Hodges, L. C. Shaffrey, A. J. Baker, and K. T. Bhatia, 2020: How important are post-tropical cyclones for European windstorm risk? *Geophys. Res. Lett.*, **47**, e2020GL089853, https://doi.org/10.1029/2020GL089853.

——, ——, ——, A. J. Baker, L. C. Shaffrey, and K. T. Bhatia, 2022: What governs the interannual variability of recurving North Atlantic tropical cyclones? *J. Climate*, **35**, 3627–3641, https://doi.org/10.1175/JCLI-D-21-0712.1.

Sarro, G., and C. Evans, 2022: An updated investigation of post-transformation intensity, structural, and duration extremes for extratropically transitioning North Atlantic tropical cyclones. *Mon. Wea. Rev.*, https://doi.org/10.1175/MWR-D-22-0088.1, in press.

Stewart, S. R., 2018: Tropical cyclone report: Hurricane Ophelia. National Hurricane Center Tropical Cyclone Rep. AL172017, 32 pp., https://www.nhc.noaa.gov/data/tcr/AL172017_Ophelia.pdf.

Studholme, J., K. I. Hodges, and C. M. Brierley, 2015: Objective determination of the extratropical transition of tropical cyclones in the Northern Hemisphere. *Tellus*, **67A**, 24474, https://doi.org/10.3402/tellusa.v67.24474.

Thorncroft, C., and K. Hodges, 2001: African easterly wave variability and its relationship to Atlantic tropical cyclone activity. *J. Climate*, **14**, 1166–1179, https://doi.org/10.1175/1520-0442(2001)014<1166:AEWVAI>2.0.CO;2.

Torn, R. D., and G. J. Hakim, 2015: Comparison of wave packets associated with extratropical transition and winter cyclones. *Mon. Wea. Rev.*, **143**, 1782–1803, https://doi.org/10.1175/MWR-D-14-00006.1.

Vidale, P. L., and Coauthors, 2021: Impact of stochastic physics and model resolution on the simulation of tropical cyclones in climate GCMs. *J. Climate*, **34**, 4315–4341, https://doi.org/10.1175/JCLI-D-20-0507.1.

Wilks, D. S., 2016: "The stippling shows statistically significant grid points": How research results are routinely overstated and over-interpreted, and what to do about it. *Bull. Amer. Meteor. Soc.*, **97**, 2263–2273, https://doi.org/10.1175/BAMS-D-15-00267.1.

Zarzycki, C. M., D. R. Thatcher, and C. Joblonowski, 2017: Objective tropical cyclone extratropical transition detection in high-resolution reanalysis and climate model data. *J. Adv. Model. Earth Syst.*, **9**, 130–148, https://doi.org/10.1002/2016MS000775.